2011 American Control Conference
on O'Farrell Street, San Francisco, CA, USA
June 29 - July 01, 2011

Adaptive Robust Control of Tracking and Synchronization for Multi-Axis Motion System

Marvin H. Cheng, *Member, IEEE* and Ezzat G. Bakhoum, *Senior Member, IEEE*

Abstract— **This paper investigates on motion synchronization of a multiple axes system. An adaptive robust control scheme was used to synthesize the synchronization compensator with cross-coupling dynamics among axes. By using the adaptive robust strategies, the asymptotic convergence of both tracking and synchronization errors are achieved. The robust control scheme also guarantees the satisfaction of transient performance, tracking errors, and synchronization errors. Experimental results of a three-axis motion system that include system uncertainties are also illustrated to verify the effectiveness of the proposed approach. The results indicate the excellent transient and both tracking and synchronization accuracies.**

I. Introduction

IN industrial manufacturing systems, such as machine tools and plotters, one often encounters situations in which two or more axes need to be coordinated. With the increasing demand of manufacturing platforms with multiple positioning components, motion synchronization of multi-axis movement has drawn much more attention recently. Such kind of synchronization requirements may be linear or rotary motions. The need for multi-axis synchronization arises whenever the axes must move together. In such kind of control applications, system performance depends more on the coordination of multiple motion actuators rather than individual motion actuators. For instance, the position coordination while moving may be required to avoid possible collision if some interlocking parts do exist in the system. These kinds of demands for improvements in system performance lead to the research activities in this area.

Since 1980s, it has been known that the coordination performance can be improved by compensating the differences in dynamics of individual actuators [1]. Nevertheless, the early researches did not take the coupling among different axes into consideration and the controllers were still synthesized independently. The diminished dimensional accuracy in those systems due to the poor synchronization of relevant axes was recognized. Therefore, different research groups have proposed various coordinating schemes and cross-coupled controllers for multiple axes to improve the synchronization accuracy. A cross-coupled controller for dual-axis feed drive systems was introduced by Koren [2] for the synchronization motion of two independent motion axes in 1980. Based on the coupling between two different axes, other approaches [3-5] were also proposed to compensate the synchronization errors in different systems. To handle more general coordinated systems in motion control, Chiu and Tomizuka [6] formulated the coordination control of multiple motion axes in a geometrical framework for three dimensional curves. With this framework, different researchers started to porpoise various cross-coupled controllers that reduce the contour error of multiple motion axes in mechanical systems. Xiao et al. [7] proposed a generalized synchronization controller for multi-axis motion system by incorporating cross-coupling technology into optimal control architecture. Jeong and You [8] applied a cascaded control structure to compensate both acceleration and position. Thus, the robustness of speed of each axis against disturbances and synchronization errors can be guaranteed. In 2003, Sun [9] applied the adaptive control method into the position synchronization of multi-robot for assembly tasks.

In this paper, we investigated the synchronization of a three actuator system. The loading of the individual axis changes under different operating conditions. As the inertia and viscous damping of the multi-axis motion system become time varying, controller with a fixed structure might not be able to provide the same performance under different operating condition. Especially, some system parameters vary while the multi-axis system is under operation. Therefore, it is necessary to develop a controller that is capable to deal with the changing parameters and still maintain the accuracy. The proposed adaptive robust controller (ARC) tries to reduce or eliminate possible uncertainties through a learning mechanism. By learning from the past information, uncertainties can be reduced and thus better performance can be expected.

The organization of this paper is as following. The modeling process is introduced in the second section. The third section describes the compensator design with the coefficient adaption. In this section, the robustness of the controlled system is also considered. An adaptive robust controller is developed in this section. The fourth section compares the results of the two synthesized controllers with the nominal plant. The experimental results of the adaptive controller are also discussed. In the last section, a summary is concluded.

978-1-4577-0079-8/11/$26.00 ©2011 AACC

II. Setup and Modeling of Motor Drive System

A. Experimental Setup

To synchronize the movements of a multi-axis motion system, different components are usually connected with a mechanical coupling. However, with the mechanical coupling, the synchronization performance cannot be guaranteed due to the distortion, backlash, or other mechanical deflects. Therefore, virtual coupling with the assistance of synchronization controller becomes popular in the past decade.

The schematic diagram of the experimental platform is shown in Figure 1. The multi-axis motion system includes three sub-systems, which are in charge of transporting a fabricating device, mechanical components, and a machining tool. Instead of synchronizing individual devices with mechanical couplings, e.g., gears, cams, and shafts, the position synchronization is realized by software algorithms. Each sub-system consists of a DC motor, which is driven by a current mode power amplifier. To setup the experimental platform, a Gateway Pentium III 700 MHz PC with 128 MB memory was used for data acquisition and implementation of the control algorithm. Two Measurement Computing DAS-1602-16 I/O boards with a 12-bit resolution D/A unit were used to send out the command signals to the motor driver. The I/O boards were also used for acquiring the measurement of the angular velocity of the roller with a 16-bit resolution of A/D. Angular position of each DC motor can be derived from individual rotary optical encoders mounted at the drive roller shaft. The resolution of each encoder is 4096 pulse/rev. The encoder is connected to a ComputerBoards PCI-QUAD04 encoder interface board. The data acquisition and control algorithm was developed using MATLAB Simulink. The Simulink model was compiled into executable binary code using an IBM ThinkPad Laptop with a 1.6 GHz PentiumM microprocessor and 2 GB memory. The real-time kernel supplied with the xPC Toolbox that comes with MATLAB R2008b is used.

B. Modeling of Mechanical Components

To design the controller for the experimental system, an accurate plant model is necessary. The nominal plant model can be obtained using well established system identification techniques. In this section, the experimental system was modeled by the block diagram shown in Figure 3. Table I summarizes the parameters of one of the individual plants.

For simplicity, it was assumed that the analog current controller is well designed and that the current loop is fast enough so that the dynamics of the current loop can be ignored. If the saturation function is ignored, the transfer function from the motor current command to the linear displacement of individual motor system can be represented by the following transfer function:

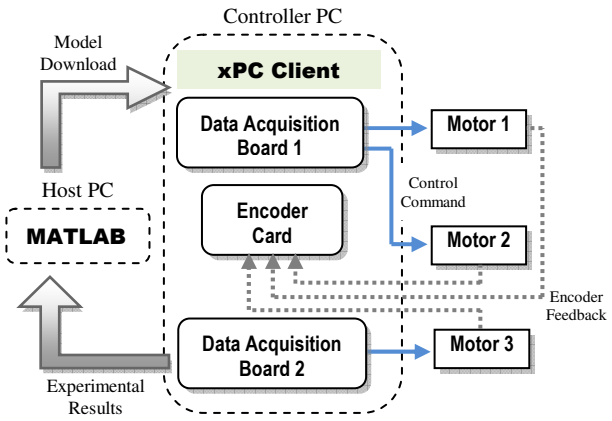

Figure 1. Schematic diagram of experimental system.

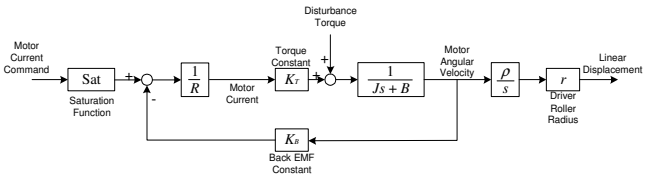

Figure 2. Schematic diagram of the motor systems.

$$G_P(s) = \frac{K_0}{s \cdot (1 + \tau \cdot s)} \tag{1}$$

where

$$K_0 = \frac{K_T \rho r}{BR + K_T K_B} \text{ and } \tau = \frac{JR}{BR + K_T K_B}. \tag{2}$$

In this case, the only parameters that need to be experimentally identified are K_0 and τ. Due to the existence of nonlinear frictions, the parameters of the system identification of the experimental results change in a range of values for each of the parameters. These two parameters are the uncertainties of the system that need to be identified for accurate position control.

TABLE I. Characteristics of the Experimental System

Description	Symbol
Effective rotational inertia	J
Effective viscous friction coefficient	B
Motor armature inductance	L
Motor armature resistance	R
Motor torque constant	K_T
Motor back-EMF constant	K_B
Gear ratio	ρ
Drive roller radius	R

C. Non-linearity and System Restrictions

The three motor systems were modeled as linear systems. While operating, there are several non-linear phenomenon need to be considered. They are: static friction and actuator saturations. As to the power saturation, the output voltage of

the adopted current amplifiers used to drive the motors saturate at ±45V.

III. Adaptive Robust Controller Design

A. System Representation of Nonlinear Terms

Based on the system description, we know that the multi-axis motion system exists with nonlinear friction uncertainties. Hence the problem formulation of individual axis can be rewritten as

$$\begin{aligned} &x_1 = \theta,\ \dot{x}_1 = x_2, \\ &\dot{x}_2 = -\frac{BR + K_T K_B}{JR} x_2 + \frac{K_T \rho}{JR}\left(v(t) - F_f(t)\right), \end{aligned} \tag{3}$$

where $v(t)$ is the control command that drives the motor to rotate. $F_f(t)$ is the bounded input disturbance due to the friction term. In the representation the inertia J and friction coefficient B are variables with bounded ranges. Thus, the equation can be expressed as

$$\dot{x}_2 = -\frac{\phi_2}{\phi_1} x_2 + \frac{K_T \rho}{\phi_1}\left(v(t) - F_f(t)\right), \tag{4}$$

where ϕ_1 and ϕ_2 are the new unknown but bounded parameters of individual axis. The unknown parameters lie in know bounded regions $\phi_1 \in [\phi_{1\min}, \phi_{1\max}]$, $\phi_2 \in [\phi_{2\min}, \phi_{2\max}]$, and $F_f \in [F_{f\min}, F_{f\max}]$. The objective of the controller design is to track the desired trajectory $x_d(t)$ and minimized the errors between the average output $x_{avg}(t)$ and the individual angular position. The initial values of ϕ_1 and ϕ_2 is determined by the nominal values of the system parameters identified.

B. Adaptive Control Laws

Define the tracking error to be the difference between the desired trajectory and the output angles as $e_i(t) = x_d(t) - x_{i1}(t)$, and the synchronization error $e_{avg,i}(t) = x_{avg}(t) - x_{i1}(t)$, where i denotes the i^{th} axis. By following the backstepping procedure of adaptive control, define

$$Z_i = \dot{e}_i + k_{p,i} e_i + k_{s,i} e_{avg,i}, \tag{5}$$

where $k_{p,i}$ and $k_{s,i}$ are the coefficient corresponding to tracking error and synchronization error of the i^{th} axis, respectively. Then, differentiating Z with respect to time leads to

$$\begin{aligned} \dot{Z}_i &= \ddot{x}_d - \ddot{x}_{i1} + k_{p,i}\dot{e}_i + k_{s,i}\dot{e}_{i,avg} \\ &= \ddot{x}_d + \frac{\phi_{i2}}{\phi_{i1}} x_{i2} - \frac{K_{T,i}\rho_i}{\phi_{i1}}\left[v_i(t) - F_{f,i}(t)\right] + k_{p,i}\dot{e}_i + k_s \dot{e}_{i,avg} \end{aligned}. \tag{6}$$

By arranging the above equation, the control input $v(t)$ can be specified as

$$v_i(t) = \frac{K_i Z_i + \phi_{i2} x_{i2} + \phi_{i1}\left(\ddot{x}_d + k_{p,i}\dot{e}_i + k_{s,i}\dot{e}_{i,avg}\right) + K_{T,i}\rho_i F_{f,i}(t)}{K_{T,i}\rho_i} \tag{7}$$

The above control input essentially guarantees the stability and ensures that $e_i(t)$ approaches to zero asymptotically. However, it should be noted that by arranging the above equation, the controller still requires explicit knowledge of the plant parameters. Thus, the control law needs to be modified as

$$v_i(t) = \frac{K_i Z_i + \hat{\phi}_{i2} x_{i2} + \hat{\phi}_{i1}\left(\ddot{x}_d + k_{p,i}\dot{e}_i + k_{s,i}\dot{e}_{i,avg}\right) + K_{T,i}\rho_i \hat{F}_{f,i}(t)}{K_{T,i}\rho_i}, \tag{8}$$

where $\hat{\phi}_{i1}$, $\hat{\phi}_{i2}$, and $\hat{F}_{f,i}$ are time-varying parameters that estimate the system parameters ϕ_{i1}, ϕ_{i2}, and $F_{f,i}$, respectively.

C. Stability and Parameter Estimation

By substituting Eq. (7) into Eq. (5), the backstepping procedure becomes

$$\dot{Z}_i = \frac{\tilde{\phi}_{i1}\left(\ddot{x}_d + k_{p,i}\dot{e}_i + k_{s,i}\dot{e}_{i,avg}\right) + \tilde{\phi}_{i2} x_{i2} + K_{T,i}\rho_i \tilde{F}_{f,i} - K_i Z_i}{\phi_{i1}}, \tag{9}$$

where $\tilde{\phi}_{i1} = \phi_{i1} - \hat{\phi}_{i1}$, $\tilde{\phi}_{i2} = \phi_{i2} - \hat{\phi}_{i2}$, and $\tilde{F}_{f,i} = F_{f,i} - \hat{F}_{f,i}$ represent the estimation errors of the time varying parameters. Thus, if a Lyapunov function V_L is defined as

$$V_L\left(Z_i, \tilde{\phi}_{i1}, \tilde{\phi}_{i2}, \tilde{F}_{f,i}\right) = \frac{1}{2}\left(\phi_{i1} Z_i^2 + \frac{\tilde{\phi}_{i1}^2}{\gamma_{i1}} + \frac{\tilde{\phi}_{i2}^2}{\gamma_{i2}} + K_{T,i}\rho_i \frac{\tilde{F}_{f,i}^2}{\gamma_{i3}}\right). \tag{10}$$

The Lyapunov function is positive definite due to the positive parameter ϕ_{i1}. The time derivative of the Lyapunov function then becomes

$$\dot{V}_L = -K_i Z_i^2 \le 0. \tag{11}$$

The derivative of the Lyapunov function is negative definite if the adaption mechanism for adjusting parameters through learning the past information are

$$\begin{aligned} \dot{\hat{\phi}}_{i1} &= -Z_i \gamma_{i1}\left(\ddot{x}_d + k_{p,i}\dot{e}_i + k_{s,i}\dot{e}_{avg,i}\right) \\ \dot{\hat{\phi}}_{i2} &= -Z_i \gamma_{i2} x_{i2} \\ \dot{\hat{F}}_{f,i} &= -Z_i \gamma_{i3} \end{aligned}, \tag{12}$$

where γ_{i1}, γ_{i2}, and γ_{i3} are all greater than zero. Since V_L is a positive definite function and $\dot{V}_L$ is a negative definite one, it follows Barbalat's lemma that Z is close to zero at infinite time. Therefore, $e_i(t)$ also decays to zero as time approaches infinite, which yields asymptotic tracking. The block diagram of the experimental setup is shown as Figure 3.

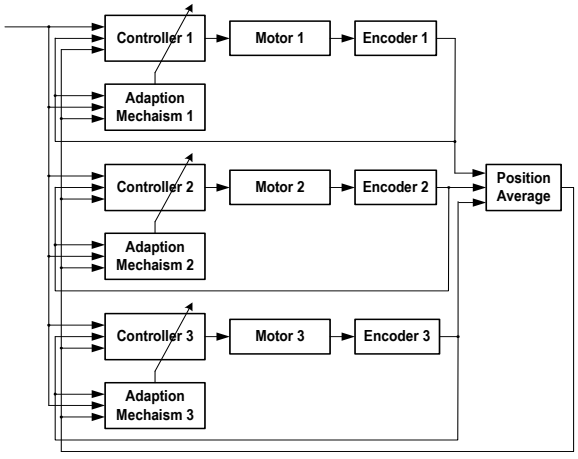

Figure 3. Block diagram of experimental system.

D. *Adaptive Robust Control*

Adaptive control has two major drawbacks: unknown transient performance and non-robustness. As the result, an adaptive controller may lead to large tracking error during the initial transient period or have a sluggish response. In addition, the parameters may be adjusted to beyond the known bounded regions. Therefore, the deterministic robust control (DRC) with the projections of parameter adaption needs to be applied to attenuate the effect the model uncertainty and improve the transient and steady-state performance.

To include the adaptive robust law in the controller, the control command $v(t)$ is modified to

$$v(t) = v_a(t) + v_s(t), \tag{13}$$

where $v_a(t)$ is the original adaptive law governed by Eq. (7) and $v_s(t)$ is the robust control effort. Apply the robust control effort to the backstepping procedure, Eq. (9) becomes

$$\dot{Z}_i = \frac{1}{\phi_{i1}}\Big[\tilde{\phi}_{i1}\left(\ddot{x}_d + k_{p,i}\dot{e}_i + k_{s,i}\dot{e}_{i,avg}\right) + \tilde{\phi}_{i2}x_{i2} + K_{T,i}\rho_i\tilde{F}_{f,i} - K_iZ_i - v_{s,i}\Big], \tag{14}$$

The essence of DRC is that the robust control input $v_{s,i}$ can be synthesized to attenuate effects of model uncertainty coming from both parametric uncertainties and nonlinearities. Thus, those requirements can be represented by the following constraints:

- $Z_i\left[\tilde{\phi}_{i1}\left(\ddot{x}_d + k_{p,i}\dot{e}_i + k_{s,i}\dot{e}_{i,avg}\right) + \tilde{\phi}_{i2}x_{i2} + K_{T,i}\rho_i\tilde{F}_{f,i} - v_{s,i}\right] \le \varepsilon$;
- $Z_iv_{s,i} \ge 0$,

where ε is a design parameter. Since ϕ_{i1} is always positive, set the Lyapunov function to be

$$V_L = \frac{1}{2}\phi_{i1}Z_i^2. \tag{15}$$

The derivative of the Lyapunov function yields

$$\dot{V}_L = -K_iZ_i^2 + Z_i\Big[\tilde{\phi}_{i1}\left(\ddot{x}_d + k_{p,i}\dot{e}_i + k_{s,i}\dot{e}_{i,avg}\right) + \tilde{\phi}_{i2}x_{i2} + K_{T,i}\rho_i\tilde{F}_{f,i} - v_{s,i}\Big] \le -K_iZ_i^2 + \varepsilon \tag{16}$$

Thus, the stability of the adaptive law can be guaranteed. The resulting adaptation law can be modified as the following projection forms. They are

$$\begin{aligned}\dot{\hat{\phi}}_{i1} &= \mathrm{proj}\left(-Z_i\gamma_{i1}\left(\ddot{x}_d + k_{p,i}\dot{e}_i + k_{s,i}\dot{e}_{avg,i}\right)\right)\\ \dot{\hat{\phi}}_{i2} &= \mathrm{proj}\left(-Z_i\gamma_{i2}x_{i2}\right)\\ \dot{\hat{F}}_{f,i} &= \mathrm{proj}\left(-Z_i\gamma_{i3}\right)\end{aligned}, \tag{17}$$

where the projection mapping proj(•) is defined as

$$\mathrm{proj}(\bullet) = \begin{cases} 0 & \text{if } \begin{cases}\hat{\phi}_{ij} = \hat{\phi}_{ij\,\max} \text{ and } \bullet > 0\\ \hat{\phi}_{ij} = \hat{\phi}_{ij\,\min} \text{ and } \bullet < 0\end{cases}\\ \bullet & \text{otherwise}\end{cases}. \tag{18}$$

As a result, the projection method guarantees that the estimated parameters stay in known bounded region all the time. It also ensures that asymptotic tracking as in adaptive control will not be lost.

The control effort $v_{s,i}$ can be designed by using the technique of completion of squares, which makes the control input becomes

$$v_{s,i} = 0.25h_iZ_i$$

$$h_i \ge \left[\frac{1}{\varepsilon_1}\phi_{i1m}^2\left(\ddot{x}_d + k_{p,i}\dot{e}_i + k_{s,i}\dot{e}_{i,avg}\right)^2 + \frac{1}{\varepsilon_2}\phi_{i2m}^2x_{i2}^2 + \frac{1}{\varepsilon_3}F_{f,im}^2\right], \tag{19}$$

where $\varepsilon = \varepsilon_1 + \varepsilon_2 + \varepsilon_3$ is the design parameter, and ϕ_{i1m}, ϕ_{i2m}, and $F_{f,im}$ are the range of the bounded parameters, respectively. With the control command, the adaptive robust control can be rewritten as

$$v_i(t) = -0.25h_iZ_i + \frac{K_iZ_i + \hat{\phi}_{i2}x_{i2} + \phi_{i1}\left(\ddot{x}_d + k_{p,i}\dot{e}_i + k_{s,i}\dot{e}_{i,avg}\right) + K_{T,i}\rho_i\hat{F}_{f,i}(t)}{K_{T,i}\rho_i} \tag{20}$$

with the adaptation mechanism. This type of controller combines the advantage of both the adaptive and robust control by using the adaption mechanism and further feedback controller v_s to improve the overall performance. Thus, the tracking error is asymptotic convergent and bounded.

IV. Experimental Results

A. *Desired Trajectory*

Due to the inherent limitation of available power inputs of control efforts, the trajectory design plays an important role to achieve the tracking and position performance. In particular, the non-parametrical uncertainties due to the quantization of digital devices might lead to large tracking errors. Such kind of non-parametrical uncertainties can make a stable system an unstable one. Therefore, to evaluate the performance of the proposed controller, each axis was set to move 30 mm. In order to minimize the overshoot, the desired trajectory was adjusted with a cycloidal increment as shown in Figure 6. Such a trajectory decreases the vibrant response during the transient.

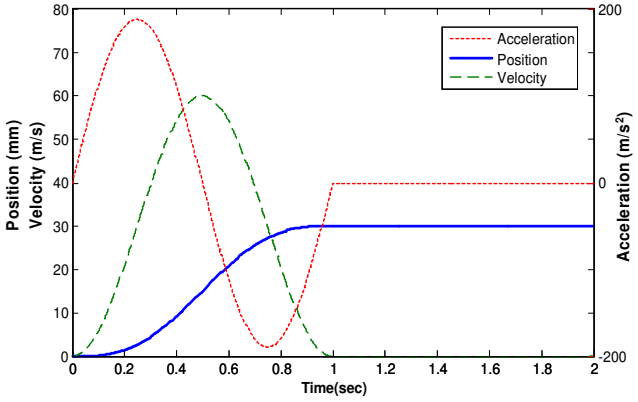

Figure 4. Desired tracking trajectory.

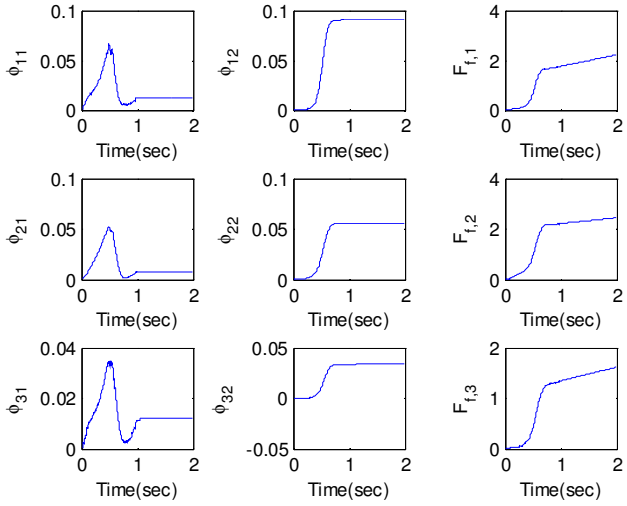

Figure 5. Parameters adaption of adaptive controller in a single run.

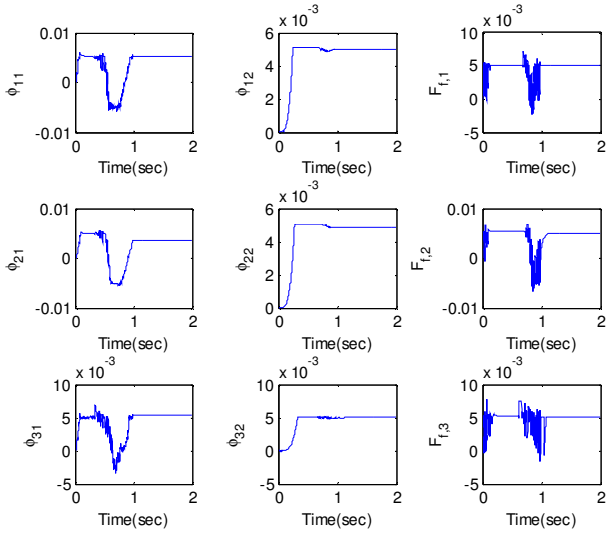

Figure 6. Parameter adaption of adaptive robust controller in a single run.

B. Controller Parameters

The controller parameters were designed by choosing $\varepsilon_1 = 0.005$, $\varepsilon_2 = 0.005$, $\varepsilon_3 = 0.005$, $k_{p1} = 40$, $k_{p2} = 35$, $k_{p3} = 35$, $k_{s1} = 30$, $k_{s2} = 25$, and $k_{s3} = 25$. Notice that the position of the movement was calculated from the measurement of the attached optical encoder measuring the angular positions. The controllers implemented need both position and velocity to be obtained at every instant of time. Because the velocity was not measured, an estimate of the velocity using the backward difference method was employed. Figure 5 and Figure 6 illustrate the adaption of the nine estimated parameters. Some of the parameters are not convergent with only the adaptive mechanism adopted. In some extreme cases or improper planned trajectory, the parameters might become divergent and yield some unstable performance due to the quantized implementation of digital devices. With the robust control scheme applied to the adaption laws, not only all the nine unknown parameters used in ARC converged to fixed values, but they were restricted within bounded regions.

C. Experimental Results

Figure 7 and 8 show the comparison of tracking and synchronization errors for the proposed trajectory using different control schemes. Both types of controllers demonstrate satisfactory performance. All the errors are bounded within ±0.4 mm.

Figure 9 shows the control efforts of the two types of controllers. To restrict the parameters within given bounds, the control commands generated in ARC algorithm fluctuate more than only the adaptive mechanism is adopted. Notice that the control commands of the adaptive controller do not converge to 0 V for individual motors, which yield that the final tracking and synchronization errors of individual axes also do not converge to zero steadily. Instead, the positions fluctuate from time to time within a small range. With the current setup, both controllers provide adequate performance for tracking and synchronization. However, if inadequate tracking trajectory is applied to the system without considering the robustness, the coefficients of adaptive controller might drift and cause unstable outputs in some cases.

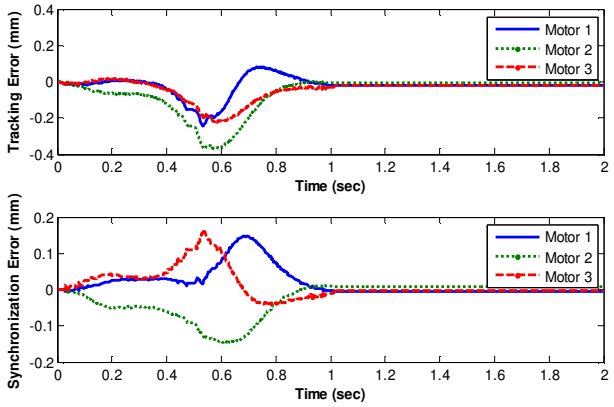

Figure 7. Performance of adaptive controller.

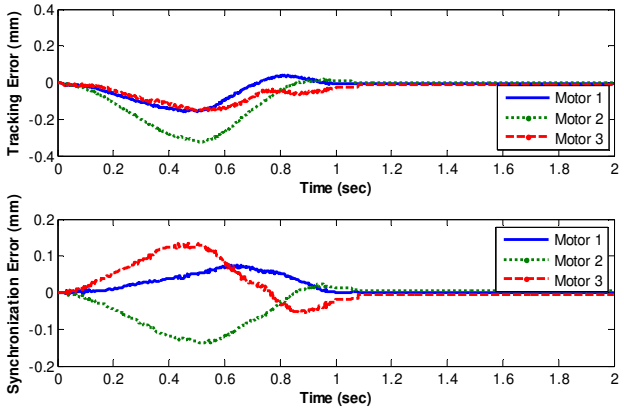

Figure 8. Performance of the adaptive robust controller.

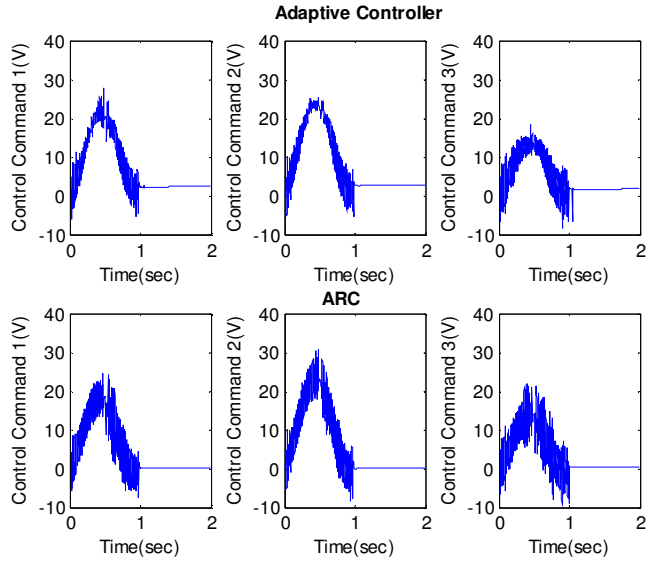

Figure 9. Control efforts of AC and ARC

Due to the friction, uncertainties, and other perturbations, the transient responses of individual movements cannot be the same. To verify the consistence and robustness of the proposed ARC controller, multiple trials of movement of the multi-axis motion system are required. Figure 10 illustrates the tracking and synchronization errors for ten trials of 30 mm movements of the system compensated by the proposed ARC controller. The experimental results demonstrate that the maximum tracking error during transient is less than 0.4 mm, and the maximum synchronization error is less than 0.2 mm. Therefore, it is clear that the experimental results promise the system specification.

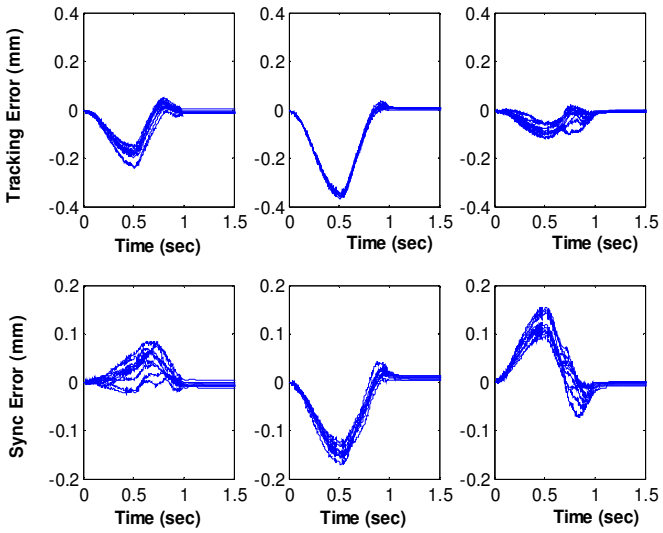

Figure 10. Tracking and synchronization errors of 10 experimental trials of ARC controller.

V. CONCLUSION

In this paper, we have presented an adaptive robust control approach with trajectory design for a multi-axis motion system. The position advance was accomplished by not violating the hardware limitation. Not only does it use robust feedback control to guarantee transient performance, tracking accuracy, and synchronization accuracy but it also applies parameter adaptation to reduce model uncertainties and improve the performance with the design of robust control. Experimental results validated the proposed approach and demonstrated excellent transient and steady state performance even though the estimated velocity was used. Besides, the control performance can be always guaranteed during the controller design procedure.

REFERENCES

[1] H. Bin, K. Yamazaki, and M. Devries, "A microprocessor-based control scheme for the improvement of contouring accuracy," Annals of the CIRP, vol. 32, pp. 275-279, 1983.

[2] Y. Koren, "Cross-coupled biaxial computer control for manufacturing systems," ASME J. of Dynamic Systems, Measurement and Control, vol. 102, pp. 265-272, 1980.

[3] M. Tomizuka, J. Hu, T. Chiu, and T. Kamano, "Synchronization of two motion control axes under adapative feedforward control," ASME J of Dynamic Systems, Measurement and Control, vol. 114, pp. 196-203, 1992.

[4] H.C. Lee and G.J. Leon, "A neuro-controller for synchronization of two motion axes," International J of Intelligent System, vol.13, pp. 571-586, 1998.

[5] H. Sun and G.T.-C. Chiu, "Motion Synchronization for Dual-Cylinder Electro-Hydraulic Lift Systems," IEEE/ASME Trans on Mechatronics, vol. 7, June 2002.

[6] G. T-C. Chiu and M. Tomizuka, "Coordinate position control of multi-axis mechanical systems," ASME J of Dynamic Systems, Measurement, and Control, vol. 120, pp. 389-393, September 1998.

[7] Y. Xiao, K. Zhu, and H. Ch. Liaw, "Generalized synchronization control of multi-axis motion systems," Control Engineering Practice, vol. 13, pp. 809–819, 2005.

[8] S.-K. Jeong and S.S. You, "Precise position synchronous control of multi-axis servo system," Mechatronics, vol. 18, pp. 129-140, 2008.

[9] D. Sun, "Position synchronization control of multiple motion axes with adaptive coupling control," Automatica, vol. 39, pp. 997-1005, 2003.

[10] M. H.-M. Cheng, A. Mitra, and C.-Y. Chen, "Synchronization Controller Synthesis of Multi-Axis Motion System," the 4th International Conference on Innovative Computing, Information and Control, Kaohsiung, Taiwan, December 2009.

[11] B. Yao and M. Tomizuka, "High Performance Robust Motion Control of Motion Tools: an Adaptive Robust Control Approach and Comparative Experiments," IEEE/ASME Transaction on Mechatronics, vol. 2, pp. 63-76, 1997.